Biophysical Journal Volume 90 May 2006 3255–3266

Monolayers of a Model Anesthetic-Binding Membrane Protein: Formation, Characterization, and Halothane-Binding Affinity

Inna Y. Churbanova,* Andrey Tronin,* Joseph Strzalka,* Thomas Gog,‡ Ivan Kuzmenko,‡ Jonas S. Johansson,† and J. Kent Blasie*

*Departments of Chemistry and †Anesthesiology, University of Pennsylvania, Philadelphia, Pennsylvania 19104-6323; and ‡Complex Materials Consortium, Advanced Photon Source, Argonne National Laboratory, Argonne, Illinois 60439

ABSTRACT hbAP0 is a model membrane protein designed to possess an anesthetic-binding cavity in its hydrophilic domain and a cation channel in its hydrophobic domain. Grazing incidence x-ray diffraction shows that hbAP0 forms four-helix bundles that are vectorially oriented within Langmuir monolayers at the air-water interface. Single monolayers of hbAP0 on alkylated solid substrates would provide an optimal system for detailed structural and dynamical studies of anesthetic-peptide interaction via x-ray and neutron scattering and polarized spectroscopic techniques. Langmuir-Blodgett and Langmuir-Schaeffer deposition and self-assembly techniques were used to form single monolayer films of the vectorially oriented peptide hbAP0 via both chemisorption and physisorption onto suitably alkylated solid substrates. The films were characterized by ultraviolet absorption, ellipsometry, circular dichroism, and polarized Fourier transform infrared spectroscopy. The α-helical secondary structure of the peptide was retained in the films. Under certain conditions, the average orientation of the helical axis was inclined relative to the plane of the substrate, approaching perpendicular in some cases. The halothane-binding affinity of the vectorially oriented hbAP0 peptide in the single monolayers, with the volatile anesthetic introduced into the moist vapor environment of the monolayer, was found to be similar to that for the detergent-solubilized peptide.

INTRODUCTION

There are different views on how inhalation anesthetics affect function of ion channels in the central nervous system, causing anesthesia. Anesthetic compounds can exert direct effects by binding to the ion channels (1,2), and indirect effects by modulating the physiochemical properties of the host lipid bilayer (3,4). Also, there is direct evidence showing that anesthetic molecules can bind to hydrophobic pockets in ligand-gated ion channels (5).

The investigation of the molecular basis of anesthetic binding to channel proteins remains a challenging task due to their complexity. Attempting to model possible targets of anesthetics in smaller, structurally defined systems, Johansson et al. employed a series of water-soluble four-helix bundle scaffolds with distinct hydrophobic cores (6–9) as a model system for studying anesthetic binding to proteins. Johansson et al. showed that anesthetic binding sites can be designed into the hydrophobic core of a water-soluble protein. The use of a water-soluble, designed protein as the model system may be considered relevant, because anesthetic molecules have been shown to bind to the hydrophobic cavities in the membrane-spanning regions of many putative candidates (10), and the hydrophobic cores of both membrane- and water-soluble proteins have been shown to be similar in terms of overall hydrophobicity (11).

Nevertheless, the application of a water-soluble model system is limited because it clearly cannot model a membrane protein in an anisotropic lipid environment, the peptide-lipid interaction possibly playing an important role in anesthetic action. As a first step, a model anesthetic-binding membrane protein was designed, designated hbAP0 (12), possessing a hydrophilic domain based on the model water-soluble, halothane-binding protein Aα_2 (7), and a hydrophobic domain based on the synthetic proton channel protein LS_2 (13). The sequence of hbAP0 is illustrated in Fig. 1. In detergent solution, hbAP0 forms four-helix bundle comprised of four identical 40-residue helices (12), each pair of helices being covalently linked via a disulfide bond between C-terminal cysteine residues to form a helix-loop-helix motif. Such dihelices could associate to form four-helix bundles of either *syn* or *anti* topology in detergent solution. Consequently, a hydrophobic cavity for binding halothane is formed by either two or four Ala residues at the same level of the core along the length of the bundle, respectively. By comparison, in the water-soluble Aα_2, the di-α-helical peptides form four-helix bundles $(A\alpha_2)_2$ with *anti* topology, with the halothane-binding cavity comprised of four Ala residues (7). Trp is located in the core of the hydrophilic domain at a level adjacent to the cavity formed by the Ala residues in both hbAP0 and Aα_2. As a result, anesthetic binding within the adjacent hydrophobic cavity can be measured quantitatively by its quenching of the Trp fluorescence.

The amphiphilic peptide hbAP0 forms a Langmuir monolayer at the air-water interface. Upon compression of the monolayer, the helices become oriented perpendicular to the interface (12). Their association in the plane of the monolayer is thereby limited to the *syn* topology, and the disulfide linkage between helices is exposed at the upper surface of the monolayer. As a result, such monolayers of the vectorially

Submitted August 11, 2005, and accepted for publication January 19, 2006.

Address reprint requests to Andrey Tronin, E-mail: tronin@sas.upenn.edu.

0006-3495/06/05/3255/12 $2.00

doi: 10.1529/biophysj.105.072348

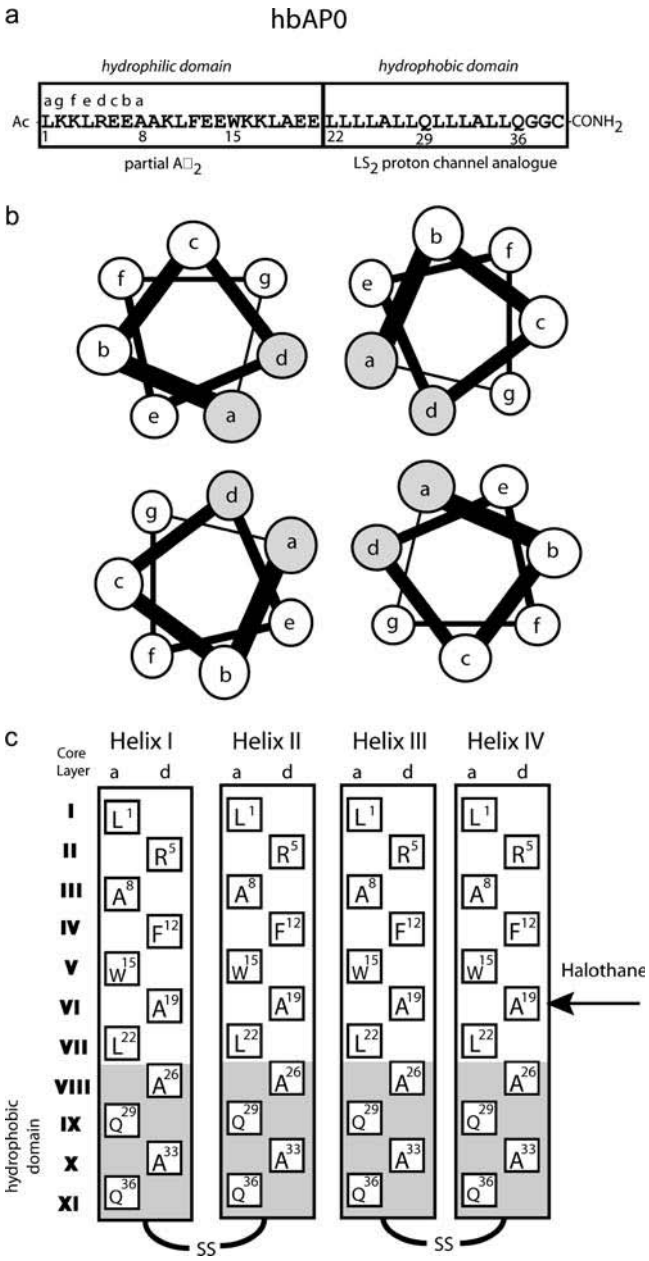

FIGURE 1 Representations of the structure of hbAP0. (*a*) Amino acid sequence, (*b*) end-on view of the four-helix bundle with each helix represented by the ''helical-wheel'' diagram, where the letters denote the seven positions within the heptad repeat, and (*c*) illustration of the interior faces of the hbAP0 amphiphilic four-helix bundle, comprised of the *a* and *d* positions in the heptad repeat at the various levels along the length of the bundle. In hbAP0, all four identical 37-residue helices are parallel or *syn*. Each pair of helices is linked via a disulfide bridge between the C-terminal cysteine residues to form a helix-loop-helix, or di-helix motif. The designed halothane binding cavity is indicated with the horizontal arrow.

oriented peptide can be used as a precursor for model membrane systems based on the vectorial incorporation of the peptide into planar lipid monolayer or bilayer systems. Furthermore, single monolayers of the vectorially oriented, amphiphilic four-helix bundle peptide on alkylated solid substrates would provide an optimal system for detailed structural and dynamical studies of anesthetic-peptide interaction via x-ray and neutron scattering and polarized spectroscopic techniques.

In this work, we show that the hbAP0 peptide associates to form four-helix bundles, with the bundle axis oriented perpendicular to the interface in Langmuir monolayers at the gas-water interface at higher surface pressures. Furthermore, we show that the disulfide linkage at the end of the hydrophobic domain of the bundle can be exploited to form vectorially oriented single monolayers of the peptide on thiol-terminated surfaces of alkylated solid substrates by either Langmuir-Schaeffer deposition from the precursor Langmuir monolayer, or even by self-assembly from either methanol or detergent solution. The affinity for halothane binding to the peptide, vectorially oriented in single monolayers in the absence of detergent, is found to be entirely similar to that for the detergent-solubilized peptide in either isotropic solution or vectorially oriented in single monolayers.

MATERIALS AND METHODS

Materials

Fluorenylmethoxycarbonyl (Fmoc)-protected L-α-amino acids, Fmoc-PEG-PAL-PS resin, hydroxydihydrobenzotriazine, and 1-hydroxybenzotriazole were purchased from Applied Biosystems (Foster City, CA). Halothane (2-bromo-2-chloro-1,1,1-trifluoroethane) was from Halocarbon Laboratories (Hackensack, NJ). *N*-octyl β-D-glucopyranoside (OG) was from Anatrace (Maumee, OH). (3-Mercaptopropyl) trimethoxysilane (MPS) was purchased from Aldrich Chemical (Milwaukee, WI). Octadecyltrichlorsilane (OTS) was obtained from HÜLS America (Bristol, PA). (3-Glycidoxypropyl) dimethylethoxysilane (GOPS) was purchased from Gelest (Morrisville, PA). All other solvents and reagents were either from Fisher Scientific (Springfield, NJ) or Sigma (St. Louis, MO).

Peptide synthesis and purification

The hbAP0 peptide was assembled on an Applied Biosystems model 433A (PerkinElmer, Foster City, CA) solid-phase protein synthesizer using the standard Fmoc/tBu protection strategy on an Fmoc-PEG-PAL-PS resin (Applied Biosystems) at 0.25-mmol scale. The peptide was acetylated at its N-terminus in 1:1 (v/v) acetic anhydride-pyridine for 30 min and purified on a reversed phase C4 high-performance liquid chromatography column (Vydac, Columbia, MD) using gradients of 6:3:1 isopropanol:acetonitrile:H_2O and water containing 0.1% (v/v) 2,2,2-trifluoroacetic acid. The pure peptide (4.56 kDa molecular mass) was dimerized by oxidizing their C-terminal cysteine residues in 1:1 (v/v) 100 mM ammonium hydrogen carbonate buffer (pH 10.0) and 2-propanol in air to form the 90-residue disulfide linked peptide dimer (9.12 kDa molecular mass). The peptide's molecular mass and purity were confirmed by matrix-assisted laser desorption/ionization mass spectrometry.

Preparation of solid substrates

For circular dichroism, ultraviolet (UV) absorption and fluorescence spectroscopy, peptide films were deposited or assembled onto quartz slides (fused silica, UV grade; 25 $\times$ 35 mm^2), which were purchased from Esco Products, Oak Ridge, NJ. For ellipsometry experiments, silicon slides (100) from Wacker (Adrian, MI) were used. Attenuated total reflection Fourier

transform infrared (ATR-FTIR) spectroscopy was performed using germanium plates from Harrick Scientific (Pleasantville, NY) ($50 \times 10 \times 2$ mm^3 with 45° beveled edges). All solid substrates were sonicated for 10 min consecutively in detergent solution, methanol, chloroform, and acetone. Silica and silicon slides were additionally cleaned in concentrated nitric acid. The slides were then rinsed with H_2O, and dried in argon. The slides were subsequently subjected to plasma cleaning for ~15 min (Harrick Scientific).

The cleaned slides were then alkylated with OTS, MPS, or GOPS. Alkylation with OTS to produce a nonpolar methyl-terminated surface was performed by sonicating the slides for 20 min in a 0.1% OTS in a solution of 80% hexadecane (99% pure), 12% carbon tetrachloride, and 8% chloroform (14). The hydrophobic domain of hbAP0 exposed at the upper surface of Langmuir monolayers at the gas-water interface at higher surface pressures might be expected to exhibit a weak van der Waals interaction with the nonpolar methyl-terminated surface of these substrates.

Alkylation with MPS to produce a thiol-terminated surface was performed using the procedure described by Goss et al. (15). A solution of 0.1 mL of MPS dissolved in 20 mL of 2-propanol was brought to reflux, the cleaned and dry substrates were immersed for 10 min and then carefully rinsed with the solvent, blown dry with a jet of argon, and cured in a drying oven at 100–107°C for 10 min. The curing step is crucial to the performance of the coupling agent. After the completion of these steps, the slides appeared as clear and clean as before the MPS treatment (16). Quartz slides alkylated with MPS were stored for a short period of time in argon. In this work, they were always exposed to the peptide for adsorption via either self-assembly or deposition within 1 h after the alkylation. Water-soluble, peptide dimers analogous to Aα_2 possessing the disulfide linkage have been shown to covalently attach to such thiol-terminated surfaces, presumably by reforming the disulfide linkage with the thiol-terminated surface (16). The disulfide linkage at the end of the hydrophobic domain of hbAP0, exposed at the upper surface of Langmuir monolayers at the gas-water interface at higher surface pressures or as available in methanol or detergent solutions of the peptide, might be expected to similarly reform a covalent disulfide linkage with the thiol-terminated surface of these substrates.

GOPS alkylation was performed in the gas phase according to protocol described in Dubrovsky et al. (17) with apparatus kindly furnished by Dr. T. Dubrovsky (BD Biosciences, San Jose, CA). Alkylation with GOPS produces a glycidyl-terminated surface. These groups react with amines of lysine residues. Lysine residues exposed at either end of the hydrophilic domain of hbAP0 might thereby provide a different mode of covalent linkage with the glycidyl-terminated surface of these substrates.

Formation of Langmuir monolayer films at the gas-water interface

Langmuir monolayers of the hbAP0 peptide were spread from methanol solution (typically ~100 μM). The aqueous subphase contained 1 mM KPi and 10 mM KCl at pH 6.7, and was maintained at constant temperature of 20°C. The peptide dissolved in methanol was spread from the meniscus of a glass capillary passing through the air/water interface at an oblique angle. After spreading, ~10 min elapsed to allow for evaporation of the solvent before compression of the monolayer to the desired surface pressure, utilizing a commercial Langmuir trough (Lauda, Lauda-Königshofen, Germany) equipped with a floating-barrier surface pressure transducer.

Deposition of Langmuir-Blodgett and Langmuir-Schaeffer films on solid substrates

Langmuir-Blodgett (L-B) deposition was utilized for the slides alkylated with OTS to possess a nonpolar methyl-terminated surface. The OTS-alkylated slide was passed vertically through the Langmuir monolayer of the peptide, compressed to 50 mN/m, and maintained at constant pressure on an aqueous subphase of 1 mM KPi and 10 mM KCl at pH 6.7 maintained at 20°C, into the subphase at speed 3 mm/min. The submerged slide was either withdrawn at the same speed through the Langmuir monolayer of the peptide at the gas-water interface resulting in the deposition of two peptide layers for study via UV absorption and fluorescence spectroscopy, or withdrawn after removal of the Langmuir monolayer of the peptide by aspiration, resulting in the deposition of only a single peptide layer for study via ellipsometry. After all such L-B depositions, the slides were stored in air.

Langmuir-Schaeffer (L-S) deposition was utilized for the slides alkylated with MPS to possess a thiol-terminated surface. The alkylated slide, oriented parallel to the surface, was lowered to bring it just into contact with a Langmuir monolayer of the peptide, compressed to 50mN/m and maintained at constant pressure on an aqueous subphase of 1 mM KPi and 10 mM KCl at pH 9.5 maintained at a constant temperature of 20°C. The slide was left in this position for ~1 h before lowering it farther through the monolayer into the subphase. After all such L-S depositions, the slides were stored in the same buffer.

Self-assembled film formation on solid substrates

For the formation hbAP0 peptide films adsorbed from solution, the lyophilized peptide was dissolved in either methanol (50 μM) or detergent solution. For the latter, the peptides were first solubilized in 4.5% (w/v) OG, 50 mM potassium phosphate (KPi), pH 8.0 buffer, and then diluted fivefold with 50 mM KPi, pH 8.0 buffer to give a final 0.9% (w/v) OG solution. The peptide solutions were filtered using Whatman (Brentford, UK) inorganic membrane syringe filters with 0.02 μm pore size. The slides, alkylated with either MPS or GOPS, were incubated overnight in these solutions and subsequently washed with water and dried under a flow of argon.

X-ray reflectivity and grazing-incidence x-ray diffraction of Langmuir monolayers at the gas-water interface

The Langmuir trough and liquid-surface spectrometer for the collection of x-ray reflectivity data from Langmuir monolayers of the hbAP0 peptide were thoroughly described previously (18) as were the reduction and analysis of the reflectivity data to provide unique electron density profiles for the peptide monolayers as a function of the surface pressure.

Grazing-incidence x-ray diffraction (GIXD) data were collected from the hbAP0 peptide monolayer at constant higher surface pressures, otherwise utilizing the same instrumentation and employing a fixed angle of incidence below the critical angle for the aqueous subphase and a charge-coupled device area detector. The specular reflectivity data $I(q_z, q_{xy} = 0\ \text{Å}^{-1})$ was attenuated with a foil strip to allow the acquisition of the GIXD data $I(q_{xy} > 0\ \text{Å}^{-1}, q_z)$ in 10-s exposures without saturation of any of the detector pixels. Comparison of subsequent time frames showed no evolution of the data indicative of the absence of radiation damage to the peptide. In addition, specular x-ray reflectivity data were collected from the peptide monolayer at constant surface pressure before and after collection of the GIXD data to verify the stability of the peptide monolayer to the GIXD data collection. Equivalent GIXD data were collected from the aqueous subphase under otherwise identical experimental conditions and used to correct the GIXD data from the peptide monolayer, via subtraction, for background scattering effects.

Ellipsometry of films on solid substrates

The thickness of the hbAP0 peptide films was determined using an AutoEl-II Null Ellipsometer (Rudolph Research, Flanders NJ) at a fixed incident angle of 70° with a helium-neon laser source ($\lambda = 632.8$ nm). All measurements were made at 25°C for the hbAP0 peptide films on silicon slides in air. All film thicknesses were calculated using the manufacturer-provided DAFIBM program using a two-layer model with uniform refractive index of 1.46 for the native silicon oxide layer and 1.5 for the alkylating and peptide layers.

Circular dichroism spectroscopy of films on solid substrates

Circular dichroism (CD) experiments were carried out with an Aviv (Lakewood, NJ) 62DS spectropolarimeter. All measurements were made at 25°C for the hbAP0 peptide films on quartz slides in air. Spectra were recorded over the far UV range of 200–260 nm with a time constant of 10 s, a spectral resolution of 1 nm, and a scan rate of 20 nm/min. The quartz slides coated with peptide films adsorbed by either self-assembly or deposition methods were positioned in the instrument with the plane of the slide oriented perpendicular to the incident measuring beam.

Infrared spectroscopy of films on solid substrates

Infrared (IR) spectra were collected with a Nicolet (Waltham, MA) Magna-IR 860 spectrometer with an ATR attachment (Harrick Scientific). All measurements were made at 25°C for the hbAP0 peptide films on germanium slides in air. Data collection parameters were set for 2 cm^{-1} resolution, and 256 scans were collected for spectra of the peptide films and background spectra of otherwise identical slides without the peptide. The infrared beam was polarized and allowed to enter the germanium plate normal to the 45° beveled edge. Parallel and perpendicular polarized attenuated total reflection infrared spectra were measured in the range 600–4000 cm^{-1}. The dichroic ratios were calculated, after background correction, for the 1657 cm^{-1} amide I band using the peak absorbance at the maximum ($R^{ATR} = A_{\parallel}/A_{\perp}$). The measured R^{ATR} values were used to evaluate average tilt angle of the helix axis in the peptide film with respect to the normal to the plane of the slide, as described in Vigano et al. (19).

Ultraviolet-visible absorption spectroscopy of films on solid substrates

UV absorption spectra were recorded with a PerkinElmer UV/vis spectrophotometer Lambda 2, equipped with a xenon short arc lamp, 150 W from Ushio America, Cypress, CA). All measurements were made at 25°C for the hbAP0 peptide films on quartz slides in air. The slides were oriented in the cuvette with their plane perpendicular with respect to the incident measuring beam. Reference baseline spectra were recorded with a similarly alkylated quartz slide without adsorbed peptide. For UV absorption, three or five slides instead of one were used to improve the quality of the spectra.

Fluorescence spectroscopy of films on solid substrates

The binding of the halothane anesthetic to hbAP0 peptide in the adsorbed films was measured by the quenching of the peptide's tryptophan fluorescence emission under a flow of mixed helium-halothane gas, either dry or moist (see below), containing increasing amounts of halothane. Tryptophan fluorescence measurements were made on quartz slides using a Shimadzu (Columbia, MD) Model RF 5301 fluorescence spectrophotometer. A homemade slide holder was inserted into a cuvette equipped for gas flow with the plane of the slide at 40° angle of incidence with respect to the excitation beam. For fluorescence spectra measurements, the peptide films were excited at 275 nm (5 nm excitation bandwidth), and the emission spectrum was recorded over the appropriate wavelength range (emission bandwidth 5 nm) at a scan step of 0.2 nm. A reference baseline spectrum was recorded with a similarly alkylated quartz slide without peptide. The temperature of the cuvette was maintained at 25°C.

Quenching data were recorded using a sequential time-frame mode. After each concentration of halothane was established, the samples were excited during sequential 3-s time-frames at 275 nm (1.5 nm excitation bandwidth) and emission was measured at 330 nm (emission bandwidth 20 nm). The fluorescence intensity was thereby found to be stable frame-to-frame at each halothane concentration, showing no decline due to photobleaching.

Halothane delivery was performed using a homemade gas mixer. Helium flow from the pressurized tank was divided into two parallel lines, and the flow in each line was regulated and controlled by a flow meter. The gas in one line was bubbled though halothane, the gas-washing bottle maintained at constant room temperature. After passing the bubbler, the two lines were reconnected, and the output mixture of pure helium with halothane-saturated helium was then also passed though a water bubbler, such that the helium-halothane mixture was subsequently saturated with water vapor for the ''moist'' case. It has been shown previously that the structure and function of membrane proteins in single monolayers and oriented multilayers are preserved under such humid inert gas conditions (20–23). The halothane concentration in the helium gas, either dry or moist, was controlled by the relative flow rate in parallel lines. To calibrate the mixer, resulting halothane concentration in the output was measured spectroscopically, using a halothane absorption line at 202 nm.

Fluorescence quenching data was first normalized by setting the initial fluorescence intensity to 1. As described previously (7,8,24), the quenched fluorescence (Q) is a function of the maximum possible quenching (Q_{max}) at an infinite halothane concentration ([Halothane]) and the affinity of halothane for its binding site (K_d) in the vicinity of the tryptophan residues. From mass law considerations, it then follows that

$$Q = 1 - Q_{max}[\text{Halothane}]/(K_d + [\text{Halothane}]). \quad (1)$$

Best-fit curves were generated using the Igor 4.09 program (WaveMetrics, Lake Oswego, OR), in which the K_d and Q_{max} are the unknown parameters. The data reported are the averages of the three experiments with separate samples.

RESULTS AND DISCUSSION

Langmuir monolayer characterization at the gas-water interface

Characterization of Langmuir monolayers of the hbAP0 peptide as a function of surface pressure by x-ray reflectivity, as described previously (18), demonstrated that the helices of the peptide were ~10 Å in diameter and ~60 Å long. At higher surface pressures above 40 mN/m, the helices are oriented with their long axis approximately perpendicular to the plane of the water-gas interface. (See Fig. 6 and associated text in Ye et al. (18).)

GIXD data, $I(q_{xy}, q_z)$, from Langmuir monolayers of the amphiphilic hbAP0 peptide and its prototype peptide, AP0 (18), at such higher surface pressures show a broad maximum for momentum transfer parallel to the monolayer plane at $q_{xy} \sim 2\pi/11$ $Å^{-1}$, which is absent in such data from the aqueous subphase itself and Langmuir monolayers of phospholipids on its surface (Fig. 2, *a* and *c*, respectively). This diffraction arises from the interference between parallel helices. The q_{xy} dependence of this GIXD data for hbAP0, which is entirely similar to that of the prototype AP0 (Fig. 2 *e*), and its inverse Fourier transform, namely the in-plane radial autocorrelation function, were modeled approximating the helices as straight rods of uniform electron density of ~6–10 Å diameter and using analytical expressions developed by Harget and Krimm (25). For AP0 and similarly for hbAP0, the modeling demonstrates that the di-helices aggregate to form four-helix bundles, which are rotationally disordered about the normal to the membrane plane with

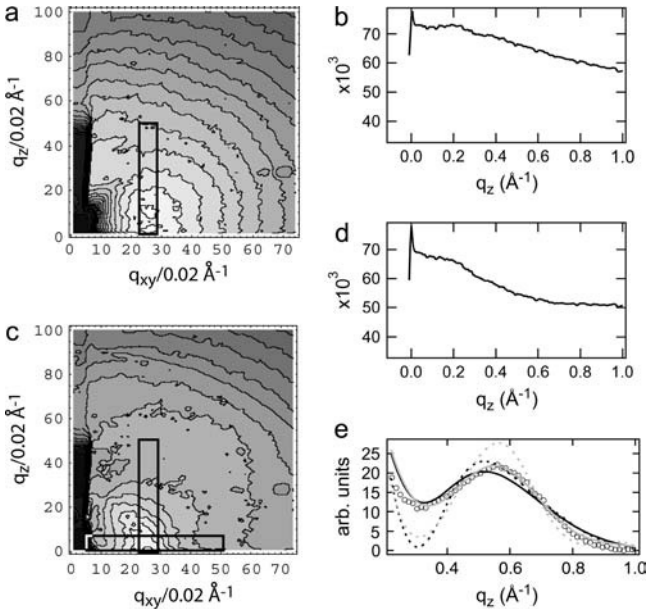

FIGURE 2 GIXD from Langmuir monolayers of amphiphilic peptide peptides at a high surface pressure. (*a*) Contour plot of experimental GIXD data from an hbAP0 monolayer corresponding to an average area/helix in the monolayer plane of 120 Å^2. (*b*) The q_z dependence of the data in *a*, integrated over the region indicated. (*c*) Contour plot of experimental GIXD data from an apo AP0 monolayer corresponding to an average area of 120 Å^2. (*d*) The q_z dependence of the data in *c*, integrated over the region indicated by the vertical rectangle. (*e*) The q_{xy} dependence of the data similar to that in *c*, integrated over the region indicated by the horizontal rectangle after subtraction of otherwise equivalent GIXD data from the surface of the clean buffer subphase (○), compared with two model calculations. Calculated q_{xy} dependence of the GIXD based on a bundle of four cylinders of 3 Å radius in a square arrangement in the plane perpendicular to the bundle axis with a nearest-neighbor separation of 11.5 Å and rotationally averaged about the bundle axis (*dashed black curve*); with the effect of convolution with the experimental Δq_{xy} resolution that broadens the maximum (*solid black curve*). Calculated q_{xy} dependence of the GIXD for a bundle of four cylinders with radius 3 Å in a 60° rhombic arrangement with a nearest neighbor separation of 12 Å, without Δq_{xy} resolution considered (*dashed shaded curve*) and with Δq_{xy} resolution included (*solid shaded curve*).

glass-like interbundle positional ordering in the monolayer plane (Fig. 2 *e*). Other possible bundles of the AP0 and hbAP0 di-helices can be readily excluded on this basis because their respective GIXD and corresponding radial autocorrelation functions differ qualitatively, well outside the signal/noise level, from their experimental counterparts. Comparison of the q_{xy} dependence of the model and experimental GIXD shown in Fig. 2 *e*, allowing for the finite Δq_{xy} resolution, provides near-perfect agreement for a four-helix bundle of ~6–6.5 Å diameter helices at a ~11–12 Å interhelix separation for the prototype peptide AP0. A rhombic arrangement of the four helices in the plane perpendicular to the bundle axis is shown to produce a better fit than a square arrangement. We note that the relatively small diameter of the best-fitting solid cylinder, i.e., 6–6.5 Å as opposed to ~10 Å, is a direct result of the dominance of the α-carbon backbone in the projection of the α-helix onto the plane perpendicular to its long axis. The q_z dependence of the GIXD data for both the hbAP0 and AP0 peptides (Fig. 2, *b* and *d*, respectively) has a primary maximum at $q_z = 0$ Å^{-1} and a weaker secondary maximum for $q_z > 0$ Å^{-1} at $q_z \sim 0.20$–0.25 Å^{-1}. The GIXD data can be analyzed in terms of Crick's analysis of the Fourier transform of coiled coils (26,27), consistent with the design of hbAP0 based on the heptad repeat. According to this analysis, the pitch P of the major helix results in diffraction described as ''layer lines'' aligned parallel to q_{xy} with a separation along q_z of 2 $\pi\ell/P$. For a four-helix bundle, the first observable layer line for $q_z > 0$ Å^{-1} would occur for $\ell = 4$. Assuming the secondary maximum off the q_{xy} axis for $q_z > 0$ Å^{-1} occurring at $q_z \sim 0.20$–0.25 Å^{-1} to be this first observable layer line from a coiled coil indicates, for a four-helix bundle, that the pitch of the major helix P is ~100–125 Å. Using an approximate value of $r \sim 5$ Å for the radius of the major helix results in a pitch-angle (given by $\tan^{-1}(2\pi r/P)$) of ~14–17°.

Adsorbed monolayer characterization

Ellipsometry and UV absorption spectroscopy

The overall quality of the hbAP0 peptide films, adsorbed via chemisorption or via L-B or L-S deposition, was monitored by both UV absorption spectroscopy and ellipsometry. Given the dimensions of the hbAP0 helix described above (~10 Å in diameter and ~60 Å long) with one Trp residue per helix, the magnitude of the UV absorption from Trp should be at the level expected for one Trp per ~100–600 Å^2 for densely packed, single monolayer films, depending on the average orientation of the helices relative to the plane of the solid substrate. Higher in-plane Trp densities would suggest multilayer film formation. whereas lesser in-plane densities would suggest less than monolayer coverage. However, Trp absorption in the UV at 280 nm was too weak to be measured reliably in such ultrathin films of the hbAP0 peptide on alkylated quartz substrates. Instead, UV absorption from the peptide bond at 220 nm was used in conjunction with a molar extinction coefficient of 21,300 M^{-1} cm^{-1} (Fig. 3). In a similar fashion, estimates of adsorbed peptide film thickness obtained via ellipsometry should be in the range of ~10–60 Å for di-helices and ~20–60 Å for four-helix bundles of hbAP0. Such measurements are only approximate due to both random and systematic errors arising from the weak UV absorbance for single monolayers of the hbAP0 peptide and the simplistic model employed for evaluation of the ellipsometry data (Table 1). Nevertheless, they were useful for establishing the incubation conditions for chemisorption of the hbAP0 peptide to thiol- and glycidyl-terminated surfaces and the conditions for L-B- and L-S-deposited hbAP0 films.

For example, in the case of chemisorption, an important parameter is the peptide concentration of the incubation

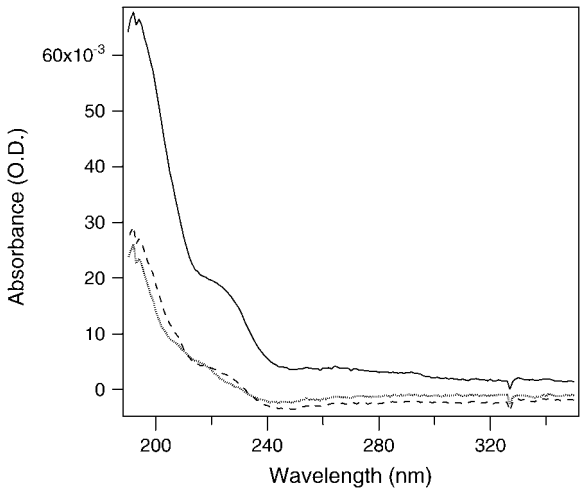

FIGURE 3 UV absorption spectra of a hbAP0 peptide film L-B deposited onto a methyl-terminated alkylated surface on quartz (*solid line*), a hbAP0 film chemisorbed onto a glycidyl-terminated alklyated surface on quartz (*dashed line*), and onto a thiol-terminated alklylated surface on quartz (*dotted line*) self-assembled from methanol solution. For UV absorption, three or five slides, coated with a film of hbAP0 on both sides, were used to improve the quality of the spectra.

solution. The dependence of film thickness on peptide concentration for self-assembly on GOPS-alkylated slides is shown in Fig. 4. For concentrations less than several micromolar, the thickness is much smaller than the dimensions of four-helix bundle, indicating poor adsorption. For a concentration of 10 μM, the thickness is comparable to the bundle size, suggesting coverage close to that for a monomolecular film. A further increase of concentration decreases the thickness. This may be due to peptide aggregation resulting in nonspecifically bound peptide that is washed off the slide after incubation. On the basis of the data shown in Fig. 4, the concentration of 10 μM peptide in the incubation solution was chosen. For the L-B and L-S film deposition techniques, important parameters are the surface pressure in the precursor Langmuir monolayer of the peptide at the gas-water interface and the pH of the aqueous subphase. For both types of deposition, film thickness reached approximate dimensions of the bundle at surface pressures of 40–50 mN/m. All films for the further study were then deposited at the surface pressure of 50 mN/m. In the case of the L-S deposition onto MPS-alkylated slides, the pH of the subphase was selected to optimize disulfide bond formation. In the case of L-B deposition onto OTS-alkylated slides, the pH of the subphase solution should approximate the isoelectric point of the peptide. The structure-based estimation of the isoelectric point of hbAP0 is ~6.2–6.7. Although there was no clear dependence of film thickness on pH over the range of 6.0–7.5, the thickness reproducibility was much better at pH = 6.5 than at lower or higher values. Hence pH = 6.5 was utilized for all subsequent L-B-deposited films for further study.

Circular dichroism spectroscopy

CD spectroscopy is more quantitative and was used to check whether the secondary structure of the peptide was preserved upon chemisorption or deposition onto the surface of the alkylated solid substrates. Fig. 5 compares the CD spectra of the hbAP0 peptide in the adsorbed films and the corresponding detergent-solution spectra. The CD spectra of both the chemisorbed and deposited films of hbAP0 generally exhibit characteristics of a predominately α-helical structure. However, the ratio of the amplitudes of the two minima at 208 and 222 nm for some of the peptide films differs somewhat from that of the isotropic solution spectrum. For α-helices, the CD absorption band at 208 nm is polarized parallel to the long axis (28–32). In our experiments, the incident light was normal to the plane of the substrate, so a relatively more negative 208 nm band suggests a more parallel average orientation of the helices with respect to the plane of the alkylated substrate surface, and a less negative 208 nm band suggests that the helices are on average tilted out of that plane (32). Thus, the helices in L-B-deposited films of hbAP0 on OTS, and in chemisorbed films on MPS assembled from detergent-solubilized hbAP0 and on GOPS assembled from methanol solution,

TABLE 1 Summary of properties* of hbAP0 monolayers

	Ellipsometry thickness (Å)	ATR-FTIR tilt angle to surface normal; dichroic ratio	Absorbance at 220 nm per monolayer; area/molecule (Å^2)	Fluorescence emission maximum (nm); intensity per monolayer	K_d (mM); Q_{max}
1. L-B deposited on methyl-terminated surface	20 ± 2	~90; 1.04 ± 0.03	0.0046; 79	325; 29	1.0 ± 0.1; 0.86 ± 0.22
2. Chemisorbed onto glycidyl-terminated surface	37 ± 11	~90; 1.03 ± 0.01	0.00382; 120	324; 35	2.4 ± 0.2; 1.26 ± 0.03
3. L-S deposited onto thiol-terminated surface	33 ± 5	50 ± 22; 1.29 ± 0.24	0.00396; 88	322; 36	–
4. Chemisorbed onto thiol-terminated surface from methanol solution	22 ± 7	51 ± 12; 1.25 ± 0.11	0.0022; 162	324; 22	3.0 ± 0.6; 1.37 ± 0.14
5. Chemisorbed onto thiol-terminated surface from detergent solution	23 ± 13	74 ± 23; 1.1 ± 0.34	0.00119; 298	320; 23	2.8 ± 0.3; 1.33 ± 0.03

*Errors indicated represent the standard deviation. All K_d and Q_{max} values shown in the last column were obtained in moist helium halothane mixtures. These values for the ''L-S deposited onto thiol-terminated surface'' case were not obtained, although for dry helium-halothane mixtures, the K_d value was found to be an order of magnitude smaller, namely 0.23 ± 0.06 mM.

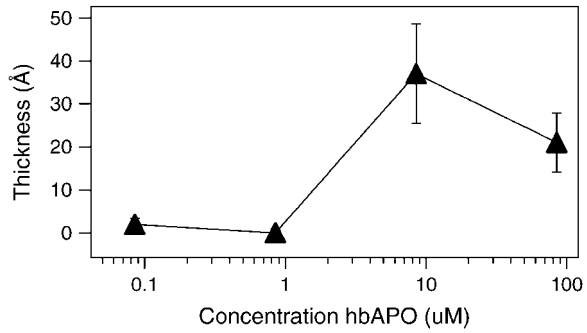

FIGURE 4 Thickness of the hbAP0 peptide layer chemisorbed onto glycidyl-terminated alkylated surfaces on silicon, as assembled from methanol solution for different concentrations of hbAP0 with incubation overnight.

appear to possess a more parallel average orientation relative to the plane of the alkylated surface, whereas the helices in chemisorbed films on MPS assembled from hbAP0 methanol solution appear to be tilted on average out of the plane of the alkylated surface.

IR spectroscopy

ATR-FTIR was used to independently check the secondary structure of hbAP0 in the adsorbed films and to provide more quantitative information on average orientation of α-helices with respect to the plane of the alkylated surface. Fig. 6 shows a typical IR spectrum of hbAP0 chemisorbed onto a glycidyl-terminated surface on germanium. The spectra of hbAP0 chemisorbed onto MPS and L-B deposited onto OTS-terminated surfaces on germanium were very similar to those shown in Fig. 6. The amide I absorption is present as a narrow band centered ~1656 cm^{-1}, confirming the predominantly α-helical structure of the peptide (30,33–35). The amide II band is present centered at 1546 cm^{-1}, also in agreement with an α-helical secondary structure (19,36). Both α-helical structure and unordered secondary structures may produce amide I type absorption near 1650 cm^{-1}, but the full width at half-height of the band is significantly narrower for the α-helical case (31). As seen in Fig. 6, the amide I band of the hbAP0 is highly symmetrical, centered at 1655 cm^{-1} with a full width at half-height of 25 cm^{-1}, indicative of a high helical content. The absorption band near 1546 cm^{-1}, which corresponds to the amide II absorption, has a noticeable shoulder that may be due to a superposition of multiple vibrational modes of lysine and tryptophan side chains (37).

Dichroism of the amide I band in the ATR-FTIR spectra provides information on the average helix orientation in the

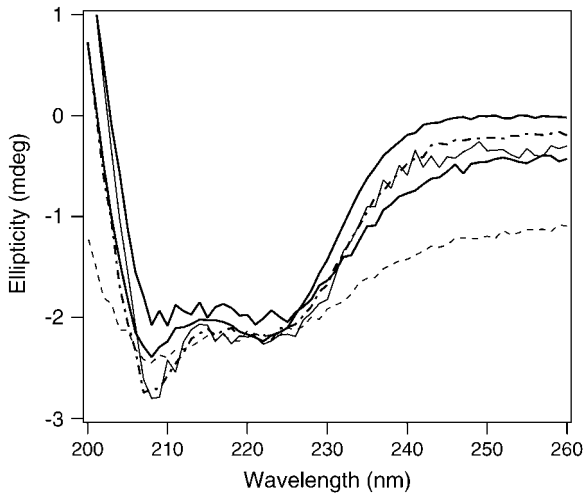

FIGURE 5 CD spectra of hbAP0 peptide layers adsorbed onto different alkylated surfaces in comparison to hbAP0 in detergent solution (50 mM KPi, pH 8.0, 0.9% OG; *solid thick line*): L-B deposited film of hbAP0 on a methyl-terminated surface of alkylated quartz (*solid thin line*); chemisorbed film of hbAP0 on a thiol-terminated surface of alkylated quartz self-assembled from either methanol solution (*dotted line*) or detergent solution (*dashed line*); chemisorbed film of hbAP0 on a glycidyl-terminated surface of alkylated quartz self-assembled from methanol solution (*dash-dot-dashed line*). The CD spectra were measured using a stack of 3–5 slides coated with a film of hbAP0 on both sides, with the plane of each slide oriented perpendicular to the measuring light beam. The scale of the solution spectrum was adjusted to compare with spectra from the slides.

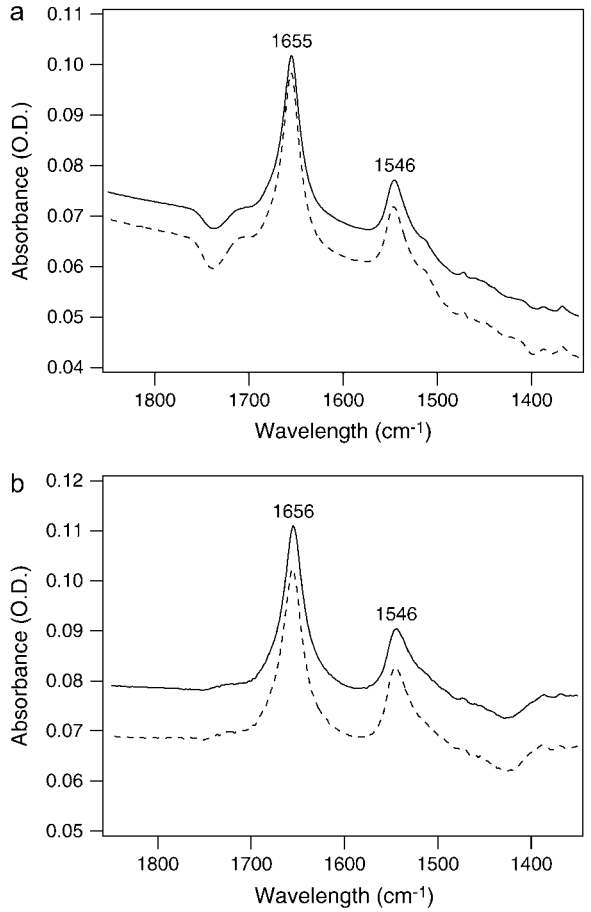

FIGURE 6 ATR-FTIR spectra of a hbAP0 film (*a*) L-S deposited onto a thiol-terminated alkylated surface on germanium and (*b*) chemisorbed from methanol solution onto a glycidyl-terminated alkylated surface on germanium. The spectra were recorded with the IR light polarized either parallel (*dashed line*) or perpendicular (*solid line*) to the plane of the surface.

peptide layer relative to the plane of the alkylated surface (36). Typical average helix tilt angles and the corresponding standard deviations, calculated from the dichroic ratio for the amide I band, are provided in Table 1, second column. As can be seen, the helices of hbAP0 are on average parallel to the alkylated surface for hbAP0 L-B deposited on methyl-terminated and chemisorbed onto glycidyl-terminated surfaces. The former case provides a dramatic example of how the average helix orientation of hbAP0 within the precursor Langmuir monolayer (e.g., perpendicular to the water-gas interface) may not be preserved upon L-B deposition onto an aklylated substrate (e.g., parallel to the plane of the alkylated surface). This may be considered as reasonable in this instance, given the weakness of the van der Waals interaction anticipated between the methyl-teminated alkylated surface and the peptide's hydrophobic domain extending over one third of the length of the four-helix bundle. The latter case involving chemisorption onto a glycidyl-terminated surface is entirely reasonable, as the lysine residues on peptide's exterior responsible for the covalent interaction are distributed over the length of the peptide's hydrophilic domain, which accounts for two-thirds of the length of the four-helix bundle. In contrast, the average orientation of the hbAP0 peptide's helices is tilted progressively more out of the plane of the alkylated surfaces for hbAP0 chemisorbed onto thiol-terminated surfaces from detergent solution, chemisorbed on thiol-terminated surfaces from methanol solution, and L-S deposited on thiol-terminated surfaces. For the latter case, some of the specimens exhibited an average helix orientation approaching normal to the alkylated surface. Note that given the coiled-coil structure of the hbAP0 4-helix bundle with a pitch-angle of 15–20°, the average tilt of the helices themselves need be only within 15–20° of the normal to the alkylated surface for the bundle axis to be perpendicular to that surface. These results are entirely reasonable, given that the cysteine residues responsible for the peptide's covalent interaction with the alkylated surface are located in a six-residue loop, joining two helices to form di-helices, at the end of the bundle's hydrophobic domain. The average tilt-angle out of the plane of the alkylated surface would be expected to vary inversely with the average area per helix in the plane of the surface. The average area/helix would then be progressively larger for the first case involving chemisorption from detergent solution (with the monolayer retaining some detergent solvating the bundle's hydrophobic domain), than for the second case involving chemisorption from methanol solution, than for the third case involving L-S deposition (in which average orientation of the helices within the precursor Langmuir monolayer is already perpendicular to the alkylated surface maintained at minimal area/helix during chemisorption). These results are also consistent with those less quantitative obtained via CD at normal incidence, as described above.

Finally, we note that it is not possible to reconcile the thicknesses of the peptide films estimated by ellipsometry with the average helix orientations within the films determined by FTIR dichroism. A minimal expectation would require qualitative agreement with larger film thicknesses corresponding to smaller average tilt angles of the helices with respect to the normal to the plane of the substrate. From Table 1 this is not the case. The errors given in Table 1 represent only the standard deviations among similarly prepared films. However, the systematic errors may be considerably larger for these measurements. In particular, the film thickness measured by ellipsometry depends on the optical model utilized. For such very thin films, simple optical models cannot account for nonuniform refractive indices within the substrate, within the adsorbed film, and across the intervening interface or for uncertainties in the real and imaginary parts of the refractive index of the film, for example. This can result in systematic errors of ~20–30 Å. Similarly, the average tilt-angle of the helices determined via dichroism of amide I IR band depends on the assumed value of angle between the peptide bond and the helical axis, which varies for different peptides, as well as on the refractive index of the film. Given the above, we take the IR dichroism measurement to provide the more reliable measurement, indicating that the helices of the hbAP0 peptide can be oriented out of the plane of the substrate, especially for the films adsorbed onto MPS-alkylated substrates via either chemisorption or L-S deposition. We plan to investigate the orientational distribution of the four-helix bundle hbAP0 peptide within such adsorbed films on solid substrate more directly by x-ray reflectivity and GIXD in the near future.

Halothane binding affinity in adsorbed monolayers

Despite being unable to reproducibly record UV absorption from the tryptophan residues in the adsorbed ultrathin films of hbAP0, the UV absorption, CD, and FTIR spectroscopy of these films clearly indicated the presence of the peptide possessing predominantly α-helical secondary structure in approximately uniform monolayer coverage of the alkylated surface. The fluorescence from the tryptophan residues could be measured reliably and used to study the halothane binding affinity of hbAP0 in the adsorbed films. Fluorescence spectra for three differently adsorbed films of hbAP0 are shown in Fig. 7. Two partially resolved emission maxima are present at ~325 nm and ~355 nm. The maximum at ~325 nm was largely predominant in the majority of adsorbed films. Its position is somewhat blue-shifted relative to that of 334 nm for the single-emission maximum, observed for the detergent-solubilized peptide (12). The emission maximum of tryptophan fluorescence can vary from 315 to 355 nm, depending on the polarity of the local environment of the residue (38,39). The two observed maxima for hbAP0 in the films are then typical for nonpolar and polar environments, respectively, providing evidence for the presence of two distinct tryptophan microenvironments in the adsorbed films. Since there are four Trp residues at the same level within the core of the hbAP0 4-helix bundle, these could represent two

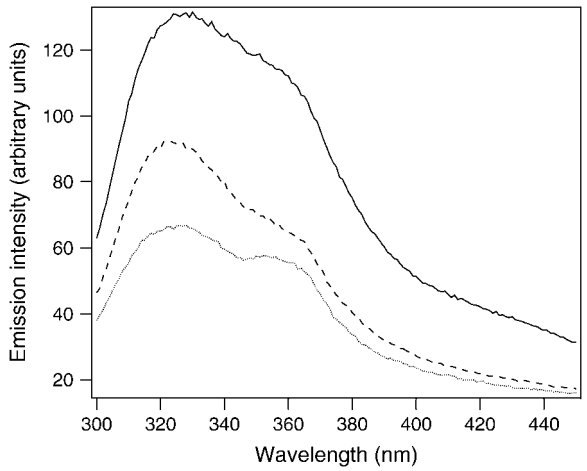

FIGURE 7 Tryptophan fluorescence emission spectra of hbAP0 peptide films L-B deposited on a methyl-terminated surface on alklyated quartz (*solid line*), chemisorbed either onto a glycidyl-terminated alkylated surface on quartz (*dashed line*) or onto a thiol-terminated alkylated surface on quartz (*dotted line*) self-assembled from methanol solution. Fluorescence spectra were measured from a single slide coated with a hbAP0 peptide film on both sides.

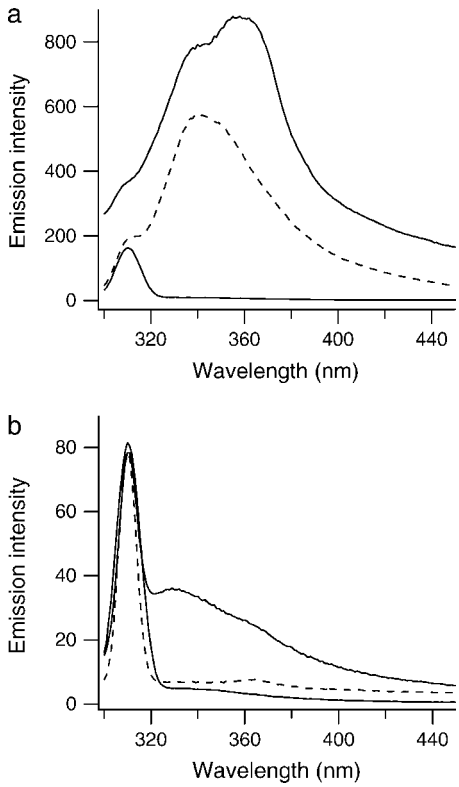

FIGURE 8 Tryptophan fluorescence emission spectra of hbAP0 peptide films L-B deposited on a methyl-terminated alkylated surface on quartz (*a*, *solid line*) and L-S deposited and chemisorbed onto a thiol-terminated alkylated surface on quartz (*b*, *solid line*), as measured in buffer (in 1 mM KPi, 10 mM KCl, pH 6.7). Also shown are the otherwise identical spectra from the buffer in the cuvette before inserting the peptide coated slide (*dotted line*) and after the slide was removed (*dashed line*). Insertion of the slide with the L-B deposited hbAP0 film on a methyl-terminated surface into the buffer results in the peptide being desorbed form the slide into the buffer (*a*), whereas insertion of the slide with the L-S deposited and chemisorbed hbAP0 film on a thiol-terminated surface does not (*b*). The emission maximum at ~310 nm is due to Raman scattering from the buffer solution.

microenvironments within the same bundle or two different microenvironments for different bundles. Given that the high α-helical content of hbAP0 is maintained upon formation of the adsorbed films, i.e., as demonstrated by circular dichhroism and FTIR spectroscopy, and the relatively large volume of the Trp residue, two microenvironments within the same four-helix bundle seem more likely, the dominant microenvironment being nonpolar as provided by the core of the hydrophilic domain of hbAP0. Some small (~2 nm) shifts of the position of the dominant emission maximum among the ultrathin films of hbAP0 adsorbed onto different alkylated surfaces (see data in Table 1) suggest some small surface-dependent changes in the conformation of the peptide.

Tryptophan fluorescence was also used to characterize the strength of the interaction of the hbAP0 peptide with the different end groups present on the alkylated surface of the substrates. For example, the van der Waals interaction was not strong enough to prevent peptide detachment from the methyl-terminated alkylated substrate surface into buffer solution, whereas the covalently bound peptide on thiol-terminated and glycidyl-terminated surfaces was much more stable. This is demonstrated in Fig. 8 for the first two cases. (The fluorescence emission from the detached peptide is seen in Fig. 8 *a* to occur at ~330 nm, indicative of a nonpolar environment for the tryptophan residues. Chemical denaturation of the AP0 and hbAP0 peptides shifts the emission maximum to longer wavelengths, indicative of a polar environment for these residues. Repeated compression-expansion cycles of the amphiphilic four-helix bundle peptides AP0 and hbAP0 in Langmuir monolayers at the air-water interface show that the peptides possess some finite solubility in the aqueous subphase. These results together suggest that the peptides enter the aqueous phase by forming some higher oligomeric aggregate, thereby preserving the nonpolar environment of the tryptophan residues instead of simply by denaturing.)

Halothane binding to the hydrophobic core of hbAP0 was monitored by the quenching of the tryptophan fluorescence. The intensity of the dominant tryptophan emission maximum versus concentration of the halothane is shown in Fig. 9. At 10 mM halothane, which is the concentration equivalent of 70% halothane saturated gas, tryptophan fluorescence was quenched almost completely. All experiments showed full reversibility of the fluorescence quenching. After the maximum halothane concentration was reached, the flow cell was purged with pure helium and the fluorescence returned to almost its initial intensity before the introduction of anesthetic. The exponential shape of the titration curves indicates that halothane was retained in the designed hydrophobic cavity of the four-helix bundle in close proximity to the tryptophan. Otherwise, in the case of collisional quenching,

the decrease of fluorescence is essentially linear. Halothane binding experiments with the analogous water-soluble four-helix bundle peptide Aα_2 showed that exponential quenching is typical for the native peptide, whereas in the presence of denaturing agents the quenching becomes linear (40,41).

Both the major and minor maxima in the fluorescence emission from the adsorbed films of hbAP0 were quenched

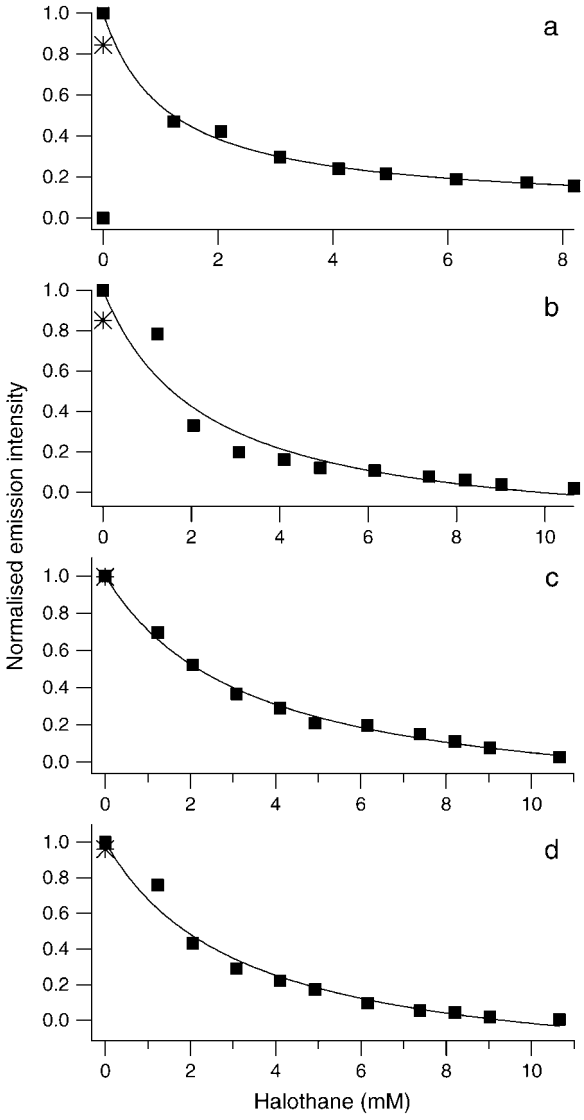

FIGURE 9 Halothane binding to the adsorbed films of hbAP0 peptide monitored by the progressive quenching of tryptophan fluorescence with increasing halothane concentration in the moist gas phase environment. (*a*) L-B film of hbAP0 deposited onto a methyl-terminated alkylated surface on quartz ($K_d = 1.0 \pm 0.1$); (*b*) self-assembled film of hbAP0 chemisorbed onto a glycidyl-terminated alkylated surface on quartz from methanol solution ($K_d = 2.4 \pm 0.2$); (*c*) self-assembled film of hbAP0 chemisorbed onto a thiol-terminated alklyated surface on quartz assembled from methanol solution ($K_d = 3.0 \pm 0.6$); and (*d*) self-assembled film of hbAP0 chemisorbed onto a thiol-terminated alklyated surface on quartz assembled from detergent solution ($K_d = 2.8 \pm 0.3$). K_d and Q_{max} are the mean of three experiments on separate specimens. The line through the data points is the best fit of Eq. 1. The fluorescence intensity after the purging with pure helium is shown by the asterisk.

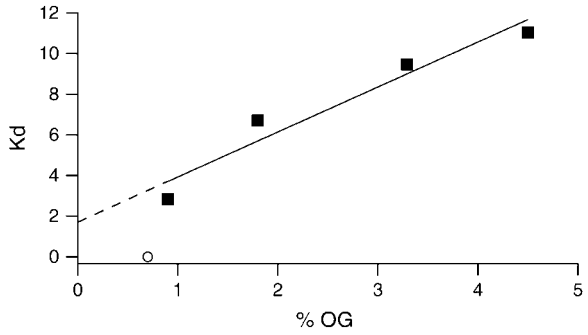

FIGURE 10 Dependence of the K_d for halothane binding to the hbAP0 peptide in detergent solution on the detergent concentration. The critical micelle concentration for the detergent (OG) is marked by an open circle. Extrapolation of the dependence to zero detergent concentration gives a K_d value of 1.7 ± 1.1 mM.

simultaneously, indicating that both populations of tryptophan were quenched by the same mechanism. This provides further support for the two microenvironments being present within the same four-helix bundle. This could require only some exposure of the indole rings of the minor population to the surface of the hydrated hydrophilic domain of hbAP0. Furthermore, this indicates that the two microenvironments do not arise from some conformational change in the bundle upon halothane binding.

The resulting dissociation constants of peptide-halothane complex within the hydrated, ultrathin films adsorbed onto different alklyated surfaces are also shown in Table 1. The affinity of the hbAP0 peptide for halothane when covalently bound to thiol- and glycidyl-terminated alkylated surfaces, namely $K_d = 2.4 \pm 0.2$ mM to 3.0 ± 0.6 mM, was about the same as for the peptide in isotropic detergent solution (0.9% OG) namely $K_d = 3.1 \pm 0.6$ mM. (12) The affinity of the peptide weakly attached to methyl-terminated alkylated surfaces was found to be ~3 times higher. Since four of the five ultrathin films of adsorbed hbAP0 contained no detergent, the effect of detergent on the K_d measured for the peptide in isotropic detergent solution was determined. The dissociation constant for halothane binding to the peptide in detergent solution, as a function of detergent concentration, is shown in Fig. 10. Extrapolation to zero detergent concentration provides a K_d value of 1.7 ± 1.1 mM. Thus, the covalent interaction of the peptide with the alkylated surfaces only slightly reduces the affinity of the peptide for the anesthetic.

CONCLUSIONS

This study demonstrates that the anesthetic-binding model ion channel peptide hbAP0 can be vectorially oriented in densely-packed, single monolayer films via covalent attachment to the thiol-terminated alkylated surfaces of solid substrates. This can be achieved via either Langmuir-Schaeffer deposition from Langmuir monolayers of the vectorially oriented amphiphilc four-helix bundle peptide or via chemisorption

of the peptide from methanol or detergent solution. The highly α-helical secondary structure of the peptide is preserved in the adsorbed monolayer films. The average orientation of the helices can approach normal to the plane of the alkylated surface in cases where the peptide residues responsible for the covalent attachment are located at one end of the four-helix bundle, as opposed to on the lateral surface of the bundle. The halothane binding affinity of the hydrophobic cavity designed into the hydrophilic domain of the peptide is similarly preserved with halothane introduction into the moist gas phase environment of the adsorbed monolayer. The conformation of the four tryptophan residues adjacent to the halothane binding cavity may be somewhat different in the adsorbed monolayers than in isotropic detergent solution. This work provides the basis for detailed structural and dynamical studies of the interaction of halothane and related volatile anesthetics with such model membrane proteins via x-ray and neutron scattering and polarized spectroscopic techniques.

This work was supported by National Institute of General Medical Sciences grant P01 GM55876. X-ray scattering experiments at the Advanced Photon Source, Argonne National Laboratory (APS/ANL) were partially supported by National Science Foundation Materials Research Science and Engineering Center grant DMR96-32598. The APS/ANL is supported by the Dept. of Energy.

REFERENCES

1. Franks, N. P., and W. R. Lieb. 1994. Molecular and cellular mechanisms of general-anesthesia. *Nature*. 367:607–614.
2. Eckenhoff, R. G., and J. S. Johansson. 1997. Molecular interactions between inhaled anesthetics and proteins. *Pharmacol. Rev*. 49:343–367.
3. Cantor, R. S. 1997. The lateral pressure profile in membranes: a physical mechanism of general anesthesia. *Biochemistry*. 36:2339–2344.
4. Hauet, N., F. Artzner, F. Boucher, C. Grabielle-Madelmont, I. Cloutier, G. Keller, P. Lesieur, D. Durand, and M. Paternostre. 2003. Interaction between artificial membranes and enflurane, a general volatile anesthetic: DPPC-enflurane interaction. *Biophys. J*. 84:3123–3137.
5. Chiara, D. C., L. J. Dangott, R. G. Eckenhoff, and J. B. Cohen. 2003. Identification of nicotinic acetylcholine receptor amino acids photolabeled by the volatile anesthetic halothane. *Biochemistry*. 42:13457–13467.
6. Zhang, T., and J. S. Johansson. 2003. An isothermal titration calorimetry study on the binding of four volatile general anesthetics to the hydrophobic core of a four-alpha-helix bundle protein. *Biophys. J*. 85:3279–3285.
7. Johansson, J. S., B. R. Gibney, F. Rabanal, K. S. Reddy, and P. L. Dutton. 1998. A designed cavity in the hydrophobic core of a four-alpha-helix bundle improves volatile anesthetic binding affinity. *Biochemistry*. 37:1421–1429.
8. Johansson, J. S., and R. G. Eckenhoff. 1996. Minimum structural requirement for an inhalational anesthetic binding site on a protein target. *Biochim. Biophys. Acta* 1290:63–68.
9. Johansson, J. S., D. Scharf, L. A. Davies, K. S. Reddy, and R. G. Eckenhoff. 2000. A designed four-alpha-helix bundle that binds the volatile general anesthetic halothane with high affinity. *Biophys. J*. 78: 982–993.
10. Johansson, J. S. 2003. Noninactivating tandem pore domain potassium channels as attractive targets for general anesthetics. *Anesth. Analg*. 96: 1248–1250.
11. Spencer, R. H., and D. C. Rees. 2002. The alpha-helix and the organization and gating of channels. *Annu. Rev. Biophys. Biomol. Struct*. 31: 207–233.
12. Ye, S. X., J. Strzalka, I. Y. Churbanova, S. Y. Zheng, J. S. Johansson, and J. K. Blasie. 2004. A model membrane protein for binding volatile anesthetics. *Biophys. J*. 87:4065–4074.
13. Lear, J. D., Z. R. Wasserman, and W. F. Degrado. 1988. Synthetic amphiphilic peptide models for protein ion channels. *Science*. 240: 1177–1181.
14. Sagiv, J. 1980. Organized monolayers by adsorption. 1. Formation and structure of oleophobic mixed monolayers on solid-surfaces. *J. Am. Chem. Soc*. 102:92–98.
15. Goss, C. A., D. H. Charych, and M. Majda. 1991. Application of (3-mercaptopropyl)trimethoxysilane as a molecular adhesive in the fabrication of vapor-deposited gold electrodes on glass substrates. *Anal. Chem*. 63:85–88.
16. Pilloud, D. L., F. Rabanal, B. R. Gibney, R. S. Farid, P. L. Dutton, and C. C. Moser. 1998. Self-assembled monolayers of synthetic hemoproteins on silanized quartz. *J. Phys. Chem. B*. 102:1926–1937.
17. Dubrovsky, T. B., M. V. Demcheva, A. P. Savitsky, E. Y. Mantrova, A. I. Yaropolov, V. V. Savransky, and L. V. Belovolova. 1993. Fluorescent and phosphorescent study of Langmuir-Blodgett antibody films for application to immunosensors. *Biosens. Bioelectron*. 8:377–385.
18. Ye, S. X., J. W. Strzalka, B. M. Discher, D. Noy, S. Y. Zheng, P. L. Dutton, and J. K. Blasie. 2004. Amphiphilic 4-helix bundles designed for biomolecular materials applications. *Langmuir*. 20:5897–5904.
19. Vigano, C., L. Manciu, F. Buyse, E. Goormaghtigh, and J. M. Ruysschaert. 2000. Attenuated total reflection IR spectroscopy as a tool to investigate the structure, orientation and tertiary structure changes in peptides and membrane proteins. *Biopolymers*. 55:373–380.
20. Pachence, J. M., P. L. Dutton, and J. K. Blasie. 1979. Structural studies on reconstituted reaction center phosphatidylcholine membranes. *Biochim. Biophys. Acta*. 548:348–373.
21. Pachence, J. M., P. L. Dutton, and J. K. Blasie. 1983. A structural investigation of cytochrome *c* binding to photosynthetic reaction centers in reconstituted membranes. *Biochim. Biophys. Acta*. 724:6–19.
22. Blasie, J. K., L. G. Herbette, D. Pascolini, V. Skita, D. H. Pierce, and A. Scarpa. 1985. Time-resolved x-ray-diffraction studies of the sarcoplasmic-reticulum membrane during active-transport. *Biophys. J*. 48:9–18.
23. Pierce, D. H., A. Scarpa, D. R. Trentham, M. R. Topp, and J. K. Blasie. 1983. Comparison of the kinetics of calcium-transport in vesicular dispersions and oriented multilayers of isolated sarcoplasmic-reticulum membranes. *Biophys. J*. 44:365–373.
24. Johansson, J. S., R. G. Eckenhoff, and P. L. Dutton. 1995. Binding of halothane to serum-albumin demonstrated using tryptophan fluorescence. *Anesthesiology*. 83:316–324.
25. Harget, P. J., and S. Krimm. 1971. Direct analysis of small-angle equatorial x-ray scattering from fibrous systems.1. Expressions for intensity and Patterson function. *Acta Crystallogr. A*. 27:586–596.
26. Crick, F. H. C. 1953. The packing of alpha-helices: simple coiled-coils. *Acta Crystallogr*. 6:689–697.
27. Crick, F. H. C. 1953. The Fourier transform of a coiled-coil. *Acta Crystallogr*. 6:685–689.
28. Moffitt, W. 1956. Optical rotatory dispersion of helical polymers. *J. Chem. Phys*. 25:467–478.
29. Olah, G. A., and H. W. Huang. 1988. Circular-dichroism of oriented alpha-helices. 1. Proof of the exciton theory. *J. Chem. Phys*. 89:2531–2538.
30. Dejongh, H. H. J., E. Goormaghtigh, and J. A. Killian. 1994. Analysis of circular-dichroism spectra of oriented protein-lipid complexes: toward a general application. *Biochemistry*. 33:14521–14528.
31. Chen, X. X., C. C. Moser, D. L. Pilloud, and P. L. Dutton. 1998. Molecular orientation of Langmuir-Blodgett films of designed heme protein and lipoprotein maquettes. *J. Phys. Chem. B*. 102:6425–6432.
32. Chen, X. X., C. C. Moser, D. L. Pilloud, B. R. Gibney, and P. L. Dutton. 1999. Engineering oriented heme protein maquette monolayers

through surface residue charge distribution patterns. *J. Phys. Chem. B.* 103:9029–9037.

33. Gray, C., S. A. Tatulian, S. A. Wharton, and L. K. Tamm. 1996. Effect of the N-terminal glycine on the secondary structure, orientation, and interaction of the influenza hemagglutinin fusion peptide with lipid bilayers. *Biophys. J.* 70:2275–2286.
34. Tamm, L. K., and S. A. Tatulian. 1993. Orientation of functional and nonfunctional PTS permease signal sequences in lipid bilayers: a polarized attenuated total-reflection infrared study. *Biochemistry.* 32:7720–7726.
35. Tamm, L. K., and S. A. Tatulian. 1997. Infrared spectroscopy of proteins and peptides in lipid bilayers. *Q. Rev. Biophys.* 30:365–429.
36. Goormaghtigh, E. C., V. Cabiaux, and J. M. Ruysschaert. 1994. Determination of soluble and membrane protein structure by Fourier transform infrared spectroscopy. III. Secondary structures. *Subcell. Biochem.* 23:405–450.
37. Barth, A., and C. Zscherp. 2002. What vibrations tell us about proteins. *Q. Rev. Biophys.* 35:369–430.
38. Reshetnyak, Y. K., Y. Koshevnik, and E. A. Burstein. 2001. Decomposition of protein tryptophan fluorescence spectra into log-normal components. III. Correlation between fluorescence and microenvironment parameters of individual tryptophan residues. *Biophys. J.* 81:1735–1758.
39. Vivian, J. T., and P. R. Callis. 2001. Mechanisms of tryptophan fluorescence shifts in proteins. *Biophys. J.* 80:2093–2109.
40. Manderson, G. A., and J. S. Johansson. 2002. Role of aromatic side chains in the binding of volatile general anesthetics to a four-alpha-helix bundle. *Biochemistry.* 41:4080–4087.
41. Manderson, G. A., S. J. Michalsky, and J. S. Johansson. 2003. Effect of four-alpha-helix bundle cavity size on volatile anesthetic binding energetics. *Biochemistry.* 42:11203–11213.